IOPscience iopscience.iop.org

Home Search Collections Journals About Contact us My IOPscience

Interaction of a phase soliton with charged impurities in a commensurate charge-density-wave system

This article has been downloaded from IOPscience. Please scroll down to see the full text article.

1991 J. Phys.: Condens. Matter 3 693

(http://iopscience.iop.org/0953-8984/3/6/007)

View the table of contents for this issue, or go to the journal homepage for more

Download details:
IP Address: 171.66.16.151
The article was downloaded on 11/05/2010 at 07:05

Please note that terms and conditions apply.

J. Phys.: Condens. Matter 3 (1991) 693–714. Printed in the UK

Interaction of a phase soliton with charged impurities in a commensurate charge-density-wave system

Boris A Malomed† and Alexander A Nepomnyashchy‡§
† P P Shirshov Institute for Oceanology, USSR Academy of Sciences, 23 Krasikov Street, Moscow 117259, USSR
‡ Institute for Mechanics of Continuous Media, Ural Branch of the USSR Academy of Sciences, 1 Academician Korolev Street, Perm, 614061, USSR

Received 15 November 1989, in final form 25 June 1990

Abstract. A model of a DC- or AC-driven underdamped or overdamped commensurate CDW system with randomly distributed charged impurities, and a similar model of a driven damped or overdamped randomly inhomogeneous long Josephson junction are considered. The models are based on an underdamped or overdamped sine–Gordon equation including a driving term and a perturbation that describes a random lattice of local impurities. The lattice may be both sparse and dense, the latter being approximated by continuous random functions. A fundamental assumption is that initially the system contains frozen solitons (kinks) trapped by a disordered potential generated by the random lattice. With increase in the DC drive, the kinks are gradually released. The corresponding current–voltage characteristics (CVCs) are found. In the underdamped version of the model, the CVC proves to be hysteretic, while the overdamped version demonstrates a very pronounced threshold field. In the underdamped model, radiative dissipation is taken into account too. A dependence of AC conductivity on the AC frequency is also found for both models.

1. Introduction

It is generally believed that the non-linear conductivity of one-dimensional metals is accounted for by the action of impurity or commensurability pinning on a charge density wave (CDW) (see the recent reviews by Grüner and Zettl (1985), Horovitz (1986), Krive *et al* (1986) and Gruner (1988)). An interesting problem is to consider a joint effect of the two pinnings. Fukuyama (1978a) was the first to attack the problem. The aim of the present paper is to obtain further insight into interaction of CDW phase solitons formed under the action of the commensurability (Rice *et al* 1976) with charged impurities.

As is usual, we take the phase of CDW in the form $\varphi = Qx + \tilde{\varphi}(x)$, where $Q = 2k_F$ is the Peierls wavenumber, and $\tilde{\varphi}(x)$ is an additional phase which varies slowly in comparison with the term Qx. The CDW is commensurable with an underlying ionic lattice if

$$Q = 2\pi(N/M)a^{-1} \tag{1.1}$$

(Lee *et al* 1974), where N and M are integers, and a is the lattice spacing. Under the condition (1.1), evolution of the phase misfit $\tilde{\varphi}(x, t)$ is governed by a perturbed sine–

§ New permanent address: Department of Mathematics, Technion, Haifa 32000, Israel.

0953-8984/91/060693 + 22 $03.50 © 1991 IOP Publishing Ltd

Gordon (SG) equation, which is a slight generalization of that put forward by Fukuyama (1978a):

$$\varphi_{tt} + M^{-1/2}\gamma\varphi_t - \varphi_{xx} + \sin\varphi + f = \sqrt{M}\,\varepsilon \sum_n \sin\left(\frac{\varphi}{M} + \theta_n\right)\delta(x - x_n) \tag{1.2}$$

where $\varphi \equiv M\tilde{\varphi}$, γ is a dissipation constant, f is the external electric field (voltage), ε is the coupling constant of the CDW to the impurities, x_n are their coordinates, and $\theta_n \equiv Qx_n$. To write equation (1.2) in terms of φ (instead of the usual phase misfit $\tilde{\varphi}$), we have performed the scale transformation $x \to \sqrt{M}x$, $t \to \sqrt{M}t$. This is the reason for appearance of the multipliers $M^{-1/2}$ and $\sqrt{M}$ in front of γ and ε in equation (1.2). If the parameters $M^{-1/2}\gamma$, f and $\sqrt{M}\,\varepsilon$ in equation (1.2) are small, a phase soliton, which is the charge carrier in the commensurate CDW system, is close in form to the unperturbed SG kink:

$$\varphi_k(x, t) = 4\tan^{-1}[\![\exp\{\sigma[x - \xi(t)](1 - v^2)^{-1/2}\}]\!]. \tag{1.3}$$

In equation (1.3), $\sigma = \pm 1$, $\xi(t) = vt$ and v are, respectively, the polarity, coordinate and velocity of the kink ($v^2 < 1$). A kink carries the electric charge

$$\sigma q \equiv 2\sigma e/M \tag{1.4}$$

e being the electron charge.

According to Weger and Horovitz (1982) and Horovitz and Trullinger (1984), in real one-dimensional metals in which the commensurability takes place, such as $NbSe_3$ and TaS, the dissipation may be very strong, so that a suitable model for them is the overdamped sine–Gordon (OSG) equation (cf equation (1.2)):

$$M^{-1/2}\gamma\varphi_t - \varphi_{xx} + \sin\varphi + f = \sqrt{M}\,\varepsilon \sum_n \sin\left(\frac{\varphi}{M} + \theta_n\right)\delta(x - x_n). \tag{1.5}$$

In the present paper we shall consider both model (1.2) and model (1.5).

A central problem of the CDW theory is the prediction of a current–voltage characteristic (CVC) (also frequently called the *I–V* characteristic), i.e. the dependence of the current j on the DC voltage f, and to find a corresponding conductivity $\rho(f) = \mathrm{d}j/\mathrm{d}f$. A well known theory of solitonic conductivity of the commensurate CDW systems has been given by Maki (1977, 1978). That theory is based on a quantum-mechanical calculation of a rate of production of kink–antikink pairs in the external DC electric field on account of the under-barrier tunnelling. The charged impurities do not play a crucial role in Maki's theory. The aim of the present paper is to elaborate in detail another model, based on the fundamental assumption that at $f = 0$ the system contains 'frozen' kinks with a finite density $n_0 \ll 1$ (this inequality guarantees that overlapping between the kinks may be neglected). According to the data available (see the above-mentioned review papers), it seems feasible that the one-dimensional metal $NbSe_3$ may be regarded as a commensurate CDW state with frozen discommensurations (kinks).

In the OSG version of the model, the kinks must be unipolar†, while in the *SG* version the presence of both polarities is possible. At $f = 0$, the frozen kinks are trapped by an effective potential relief generated by the impurities. It is commonly assumed that distribution of the impurities is random (Fukuyama and Lee 1978), so that the potential

† Of course, in this case the CDW conductor does not bear a net electric charge: the charge density $\sigma q n_0$ of the kinks (see equation (1.4)) is compensated by charge of the electrons in the valence band.

relief is disordered (previously, the effect of a disordered potential on an incommensurate CDW was studied by Efetov and Larkin (1977)). On increase in the voltage f, the trapped kinks will be released gradually (a conductivity model based on electric-field depinning of an *incommensurate* CDW has been given in detail; see the paper by Lee and Rice (1979) and the review by Grüner and Zettl (1985)). These are only the free (released) kinks which contribute to the conductivity. If $n_t(f)$ is the density of kinks which remain in a trapped state at a given f, the CVC takes the form

$$j = qv(f)[n_0 - n_t(f)] \tag{1.6}$$

where $v(f)$ is a mean velocity of a free kink. The main non-linearity of a corresponding conductivity is due to the dependence $n_t(f)$.

An important parameter of the model is a mean distance l between the impurities. According to Fukuyama (1978a), in a realistic model $l \ll 1$. In this case, taking account of the random distribution of x_n, it seems natural to approximate the right-hand sides of equations (1.2) and (1.5) as follows:

$$\sqrt{M}\varepsilon \sum_n \cos\left(\frac{\varphi}{M} + Qx_n\right)\delta(x - x_n) \rightarrow \zeta_1(x)\sin\left(\frac{\varphi}{M}\right) + \zeta_2(x)\cos\left(\frac{\varphi}{M}\right) \tag{1.7}$$

where $\zeta_1(x)$ and $\zeta_2(x)$ are Gaussian random functions subject to the correlations

$$\langle\zeta_1(x)\rangle = \langle\zeta_2(x)\rangle = \langle\zeta_1(x)\zeta_2(x')\rangle = 0 \tag{1.8}$$

$$\langle\zeta_1(x)\zeta_1(x')\rangle = \langle\zeta_2(x)\zeta_2(x')\rangle = \tilde{\varepsilon}^2\delta(x - x') \tag{1.9}$$

where $\tilde{\varepsilon}^2 \equiv M\varepsilon^2/2l$ will also be regarded as a small parameter. A different but similar approximation of equation (1.2) was employed by Fukuyama (1978a). In the present paper, we shall consider both the cases $l \ll 1$ (in the approximation (1.7)) and $l \gg 1$ (based on the original equations (1.2) or (1.5)), in order to demonstrate that general consequences of the underlying idea that the kinks trapped initially by the disordered potential are released gradually when increasing in the DC voltage f are insensitive to details of the model. In particular, in the OSG model the conductivity demonstrates a very pronounced threshold, the threshold voltage strongly depending on the concentration l^{-1} of the impurities. In the SG model, the threshold voltage is very small; at the same time, a noticeable feature of its CVC (I–V characteristic) is the presence of a large hysteresis. The discrete models (1.2) and (1.5) with $l \gg 1$ are considered in section 2, and the corresponding continuum models, based on the approximation (1.7), are considered in section 3†.

If the dissipation constant γ in the SG model is sufficiently small, the dependence $v(f)$ and, hence, the CVC defined by equation (1.6) may be significantly affected by radiative losses (emission of quasi-linear waves by the kink moving through the random array of impurities). The radiative losses are analysed (for both cases $l \gg 1$ and $l \ll 1$) in section 4.

Finally, section 5 is devoted to calculation of the AC conductivity in the case when the AC voltage

$$f(t) = F\cos(\omega t) \tag{1.10}$$

is applied to the system. In the framework of the pair production model, the AC conductivity was calculated by Maki (1978) too. In our model, the calculation is based on

† The main results of investigation of the continuum model have been previously reported in a brief form by Malomed (1989).

the obvious idea that, under the action of the AC voltage, the trapped kinks perform small oscillations near minima of the disordered trapping potential. We develop the analysis for both cases $l \gg 1$ and $l \ll 1$ within the framework of both the SG and the OSG models.

In concluding section 6, we briefly discuss general qualitative predictions following from our model, and possibilities of their experimental verification. However, a detailed comparison of the CVCs obtained in the present work (and of those found earlier by Malomed (1988, 1989)) with experimental I–V characteristics of the CDW systems which are likely to be commensurate is deferred to another paper.

To conclude the introduction, we comment on the commensurability index M; see equation (1.1). As is well known, the phase solitons may occur in systems with $M \geqslant 3$. At the same time, $M = 1$ and $M = 2$ may be induced if an external spatially periodic electric field (generated by an ionic superlattice) is imposed upon an incommensurate CDW system. The cases $M = 1$ and $M = 2$ were discussed, respectively, by Grüner *et al* (1981), Hansen and Carneiro (1984), Apostol and Baldea (1985) and Fukuyama (1978b). In particular, arguments were given in favour of the presence of such ionic superlattices in the one-dimensional metal compounds KCP (Fukuyama 1978b, Apostol and Baldea 1985) and $NbSe_3$ (Grüner *et al* (1981). Hansen and Carneiro (1984) and Apostol and Baldea (1985) emphasized that the ionic superlattice might contain a random component together with the regular component. While the regular component gives rise to the term $\sin\varphi$ in equations (1.2) and (1.5), the random component generates the right-hand sides of these equations. Also, the case $M = 2$ takes place if the interaction of phonons of two sorts with a CDW is taken into account (Horovitz 1986). So, all the values $M \geqslant 1$ are physically meaningful. The model (1.2) with $M = 1$ was studied in detail previously by one of the present authors (Malomed 1988). In the present paper we concentrate on the discrete models (1.2) and (1.5) with $M \geqslant 2$. As for the continuum model (1.7), all results can be obtained in a general form, i.e. without specifying the value of M. Finally, it is noteworthy that the continuum models (1.2) and (1.7) with $M = 1$, $\zeta_2 \equiv 0$, describes a damped driven long Josephson junction (LJJ) with the maximum supercurrent density subject to a random spatial modulation (Mineev *et al* 1981); an analogy between a CDW system with impurities and an inhomogeneous LJJ was discussed by Barnes and Zawadowski (1983). At the same time, the models (1.5) and (1.7) with $M = 1$, $\zeta_2 = 0$, describe a randomly inhomogeneous LJJ of SNS type, i.e. two bulk superconductors separated by a thin layer of a normal metal. In section 3, we discuss applications of the obtained results to the LJJ theory.

2. The discrete model ($M \geqslant 2$)

In the case $l \gg 1$, CVC and other dynamical characteristics are determined by interaction of a soliton with an individual impurity. As is seen from equation (1.2), this interaction is described by the Hamiltonian

$$H_{\text{int}} = M^{3/2}\varepsilon\{1 + \cos[\varphi(x_n)/M + \theta_n]\}. \tag{2.1}$$

Inserting the kink's waveform (1.3) (with $v = 0$) into equation (2.1), we find, in the spirit of the perturbation theory for SG solitons (Fogel *et al* 1976, McLaughlin and Scott 1978, the effective potential of the kink–impurity interaction:

$$U_M(\xi) = M^{3/2}\varepsilon[\![1 + \cos\{(4/M)\tan^{-1}[\exp(-\sigma\xi)] + \theta_n\}]\!] \tag{2.2}$$

where ξ represents, in fact, $\xi - x_n$. Depending on the value of the phase parameter θ_n,

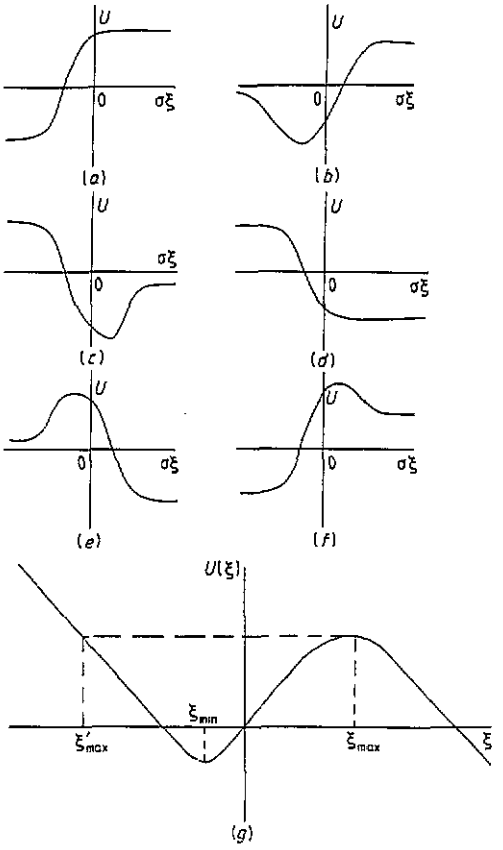

Figure 1. The shape of the potential (2.2). (*a*) $0 < \theta_n < \pi - 2\pi/M$; (*b*) $\pi - 2\pi/M < \theta_n < \pi - \pi/M$; (*c*) $\pi - \pi/M < \theta_n < \pi$; (*d*) $\pi < \theta_n < 2\pi - 2\pi/M$; (*e*) $2\pi - 2\pi/M < \theta_n < 2\pi - \pi/M$; (*f*) $2\pi - \pi/M < \theta_n < 2\pi$. (*g*) A typical kink-trapping well in the kink's effective potential $U(\xi)$ 'tilted' on account of the additional term $-2\pi f\xi$.

the potential (2.2) takes one of the forms shown in figure 1. As we see, the potential has no more than one extremum (unlike this, in the case $M = 1$ the potential has two extrema; see the paper by Malomed (1988)). In particular, at $M = 2$ an explicit form of the potential (2.2) is

$$U_2(\xi) = 2^{3/2}\varepsilon[1 + \cos\theta_n \tanh(\sigma\xi) - \sin\theta_n \operatorname{sech}(\sigma\xi)] \tag{2.3}$$

(in the case $M = 2$, the configurations in figures 1(*a*) and 1(*d*) are absent).

At $f = 0$, a kink may reside either in a potential well (figures 1(*b*) and 1(*c*)) or in a wide potential valley bounded by the potential steps (figures 1(*e*) and 1(*f*)). On increase in f, a trapped kink escapes at an inflection point ξ ($U''(\xi_{\text{inf}}) = 0$) when, for a given θ_n,

$$2\pi f + U'(\xi_{\text{inf}}) = 0 \tag{2.4}$$

($2\pi f$ is the driving force acting upon the kink). In particular, for $M = 2$, equations (2.4) and (2.3) yield

$$\sinh\xi_{\text{inf}} = \tan(\theta_n/2) \qquad f = (\sqrt{2}\,\varepsilon/\pi)\cos^2(\theta_n/2). \tag{2.5}$$

To find the density $n_t(f)$ of the trapped kinks which determines the CDC (1.6), it is necessary to calculate the share $\nu(f)$ of the trapped states that have disappeared on increase in the DC voltage from zero to a given value f. In other words, $\nu(f)$ is the share of the points ξ_{cf} for which $|U'(\xi_{\text{inf}})| < 2\pi f$. To perform this calculation, we assume,

according to above, that the parameter θ_n is a random quantity distributed randomly over the interval $(0; 2\pi)$. Lengthy but straightforward calculations following the lines of the paper by Malomed (1988) (where the same problem has been solved for $M = 1$) yield the following results†. First of all, it is convenient to introduce the renormalized DC voltage

$$g = \pi f/\sqrt{M}\,\varepsilon \tag{2.6}$$

and the function $\theta(g)$ defined implicitly by the equations

$$\theta(g) = \pi - (2/M)\sin^{-1}(\operatorname{sech}\xi) - \sin^{-1}[1 + (M/2)^2 \sinh^2\xi]^{-1/2} \tag{2.7a}$$

$$g = \operatorname{sech}\xi\,[1 + (M/2)^2 \sinh^2\xi]^{-1/2}. \tag{2.7b}$$

In fact, the auxiliary parameter ξ in equations (2.7) has the sense of $\xi_{\inf}$, so that in the case $M = 2$ these equations are equivalent to (2.5). The function $\theta(g)$ decreases in a monotonic fashion from $\theta(0) = \pi$ to $\theta(1) = \pi(M-2)/2M$ when g increases from 0 to 1.

We shall also need the parameters g_1 and g_2 defined by the equations $\theta(g_1) = \pi(M-1)/M$ and $\theta(g_2) = \pi(M-2)/M$ $(g_1 < g_2 < 1)$. Then an expression for the above-mentioned share $\nu(g)$ of the depinned states can be written in the following form. In the interval $0 < g < g_1$,

$$\nu_M(g) = \tfrac{1}{2}[(3M-1)/(M+1)][\pi - \theta(g)]. \tag{2.8a}$$

In the interval $g_1 < g < g_2$,

$$\nu_M(g) = (3M-1)/2M(M+1) + \tfrac{1}{2}[(5M-3)/(M+1)][\pi(M-1)/M - \theta(g)]. \tag{2.8b}$$

In the interval $g_2 < g < 1$,

$$\nu_M(g) = 2(2M-1)/M(M+1) + (2/\pi)[(M-1)/(M+1)][\pi(M-2)/M - \theta(g)]. \tag{2.8c}$$

In the particular case $M = 2$, the dependence $\nu(g)$ defined by equations (2.7) and (2.8) is simpler. In the interval $0 < g < \frac{1}{2}$,

$$\nu_2(g) = (\tfrac{5}{3}/\pi)\sin^{-1} g^{1/2}. \tag{2.9a}$$

In the interval $\frac{1}{2} < g < 1$,

$$\nu_2(g) = -\tfrac{1}{6} + (\tfrac{7}{3}/\pi)\sin^{-1} g^{1/2}. \tag{2.9b}$$

Finally, it is easy to find $\nu(g)$ for $M = \infty$. Indeed, in this limiting case there only remain the two configurations in figures 1(*a*) and 1(*d*) of the effective potential (2.2), $\xi_{\inf} = 0$, and a relation between g and θ analogous to (2.5) and (2.7) takes the form $g = \sin\theta$, i.e. $\theta = \pi - \sin^{-1} g$. Eventually, we obtain

$$\nu_\infty(g) = (2/\pi)\sin^{-1} g. \tag{2.10}$$

Finally, it follows immediately from equations (2.2) and (2.4) that there remains no trapped state at $g > 1$, so that in this range

$$\nu_M(g) = 1. \tag{2.11}$$

The dependence $\nu_M(g)$ for $M = 2, 3, 4$ and ∞ are shown in figure 2. As we see, all the graphs are fairly close. According to equations (2.8)–(2.11), the full curve $\nu_M(g)$ has

† These results have been obtained in the one-kink approximation, which is valid under the condition $ln_0 \ll 1$ (one kink per many impurities). Otherwise, many-kink contributions will be essential.

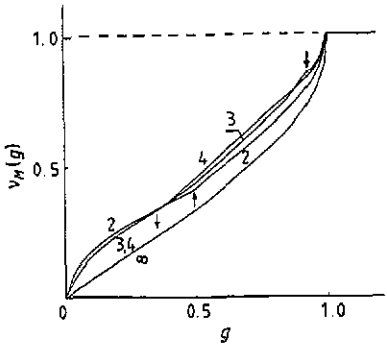

Figure 2. The dependences $\nu_M(g)$ defined by equations (2.6)–(2.11). The arrows ↑ and ↓ respectively indicate the breaks of the graphs for $M = 2$ and $M = 3$ (apart from the common break at $g = 1$). The curves for $M = 2$ and $M = 3$ are indistinguishable in the range $g < 0.3$.

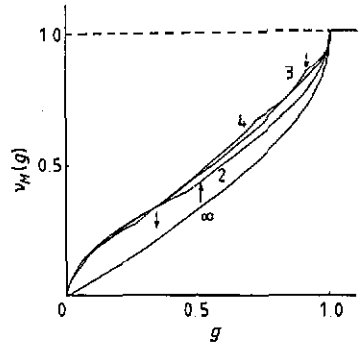

Figure 3. The corrected dependence $\nu_M(g)$ defined by equations (2.13) and (2.14). The arrows ↑ and ↓ have the same meaning as in figure 2.

two breaks at $g = \frac{1}{2}$ and $g = 1$ for $M = 2$, three breaks at $g = g_1$, $g = g_2$ and $g = 1$ for $3 \leqslant M < \infty$, and a single break at $g = 1$ for $M = \infty$. In any case, the derivative $d\nu/dg$ diverges at $1 - g \to +0$:

$$d\nu/dg \sim (1-g)^{-1/2}. \tag{2.12}$$

The breaks at the points g_1 and g_2 are scarcely conspicuous.

The model considered also has a different version which yields slightly different results. If we take into account quantum tunnelling of the trapped kinks (Maki 1977, 1978, Krive *et al* 1987), it is natural to expect that, during a sufficiently long time, the kinks located to the left of the potential hump in figure 1(*e*) or to the right of that in figure 1(*f*) will tunnel under a hump and find themselves in a neighbouring valley corresponding to a lower-energy level. This implies that, at $f = 0$, the kinks may reside either in a potential well (figure 1(*b*) and 1(*c*)) or in a valley bounded by the potential steps in figure 1(*a*) or 1(*f*) from the right, and by those in figure 1(*d*) or 1(*e*) from the left. With regard to this, equations (2.8*a*)–(2.8*c*) are replaced, respectively, by the following:

$$\nu_M(g) = \rho_1[\pi - \theta(g)] \tag{2.13a}$$

$$\nu_M(g) = (\pi/M)\rho_1 + (\rho_1 + \rho_3)[\pi(M-1)/M - \theta(g)] \tag{2.13b}$$

$$\nu_M(g) = (\pi/M)(2\rho_1 + \rho_3) + 2\rho_2[\pi(M-2)/M - \theta(g)] \tag{2.13c}$$

where $\rho_1 \equiv (3M+1)(2M-1)(4\pi M)^{-1}(M+1)^{-1}$, $\rho_2 \equiv (16M^2 - 15M - 7)\ (16\pi M)^{-1}(M+1)^{-1}$, $\rho_3 \equiv 3(5M^2 - 5M - 2) \times (16\pi M)^{-1}(M+1)^{-1}$, and the function $\theta(g)$ and the quantities g_1 and g_2 are the same as above. In the case $M = 2$, equations (2.13) simplify to (cf (2.9))

$$\nu_2(g) = (\tfrac{1}{4}/\pi)\sin^{-1} g^{1/2} \tag{2.14a}$$

for $0 < g < 1/2$ and to

$$\nu_2(g) = -\tfrac{1}{8} + (\tfrac{3}{4}/\pi)\sin^{-1} g^{1/2} \tag{2.14b}$$

for $\frac{1}{2} < g < 1$. The dependences (2.13) and (2.14), together with (2.10) (which is,

evidently, the same in both versions of the model) are shown in figure 3 (with regard to (2.11)). If we compare figure 3 with figure 2, no real difference between the two versions is obvious.

It is pertinent to compare the present results with those obtained by Malomed (1988) for $M = 1$ (in that paper, the effect of the under-hump tunnelling was taken into account). The dependence $\nu_1(g)$ is, as a whole, similar to $\nu_M(g)$ for $M \geqslant 2$. In particular, at $1 - g \to +0$ the derivative $d\nu_1/dg$ diverges according to equation (2.12), and the graph $\nu_1(g)$ demonstrates a break at $g = 4 \times 3^{-3/2}$ (apart from the break at $g = 1$).

The central point of the subsequent analysis is to relate the density $n_0 - n_t$ of the free kinks to the quantity $\nu(g)$. This relation proves to be different in principle in the SG and OSG models. A fundamental reason for the difference is the following: in the SG model, a characteristic critical field $\sim \varepsilon$ providing the release of a pinned (trapped) kink is much greater than the minimum value (about $\gamma\sqrt{\varepsilon}$; see below), admitting free motion of the kink (McLaughlin and Scott 1978) so that a kink, once released, will remain free; in the OSG model, where the kink's law of motion is purely dissipative, a released kink will be pinned again by any vacant potential well. Therefore, the OSG model becomes conductive at a value of f at which the density of pinned states, which decreases on increase in f, becomes equal to the density of kinks (Malomed 1988, 1989). In the SG model, the threshold for the onset of conductivity is much lower. At the same time, in the SG model, collisions between free and pinned kinks must be taken into account. Let us now proceed with the details of the calculations.

2.1. *The SG model*

It is natural to expect that in the SG model (1.2) the density of free kinks is related to the share $\nu(g)$ of the released pinned states as follows: $n_0 - n_t = n_0\nu(g)$ (recall that n_0 is the total density of the kinks in the system). Insertion of this relation into equation (1.6) immediately yields the CVC (Malomed 1988)

$$j = qv(f)n_0\nu(g). \tag{2.15}$$

The velocity $v(f)$ of a free kinks is given by the well known expression of McLaughlin and Scott (1978):

$$v(f) = [1 + (4\tilde{\gamma}/\pi f)^2]^{-1/2} \tag{2.16}$$

where $\tilde{\gamma} \equiv M^{-1/2}\gamma$ (see equation (1.2)).

Strictly speaking, equation (2.16), as well as (2.20) (see below), pertains to the homogeneous system ($\varepsilon = 0$). However, it will be seen that in all cases of interest they are surely relevant as expressions for a mean velocity, except for the range of small f, $f \leqslant \gamma\sqrt{\varepsilon}$. In that range, the moving kinks are captured by potential traps in the form of steps (figures 1(*a*) and 1(*d*)) and humps (figures 1(*e*) and 1(*f*)). This means that solitonic conductivity is absent unless the voltage exceeds a threshold value $f_0 \sim \gamma\sqrt{\varepsilon}$. Under the condition $\sqrt{\varepsilon} \gg \gamma$, the value f_0 can be found in an accurate form from the energy equation $4v^2 = (\pi f/2\gamma)^2 = U_{\max}$, $U_{\max}$ being a maximum height of the potential hump (McLaughlin and Scott 1978) (see also the papers by Sakai *et al* (1987) and Malomed (1988)). It is easy to find that $U_{\max} = 2M^{3/2}\varepsilon \sin^2(\pi/M)$ for $M \geqslant 2$ ($U_{\max} = 2\varepsilon$ for $M = 1$), so that

$$f_0^2 = (8/\pi^2)M^{3/2}\tilde{\gamma}^2\varepsilon \sin^2(\pi/M). \tag{2.17}$$

Equation (2.16) for the CVC is valid if collisions with the free kinks do not result in release of the trapped (pinned) kinks, i.e. the collisions do not alter the density of the

free kinks. Let us analyse the collisions in some detail in order to find conditions which guarantee that this important assumption holds indeed.

In the presence of the external force (voltage) f, the potentials shown in figure 1 become 'tilted' because the term $-2\pi f\xi$ must be added to the kink's potential energy (2.2). A typical well trapping a kink in the tilted potential is shown in figure 1(g). The trapped kink rests at the potential minimum $\xi = \xi_{\min}$.

In the lowest approximation, the collision of a trapped kink with a free kink moving with a velocity v results in a rapid shift of the coordinate ξ of the trapped kink by the amount (Zakharov *et al* 1980)

$$\Delta\xi = \pm \log[(1 + \sqrt{1 - v^2})^2/v^2].$$

The trapped kink shifts to the left (from the viewpoint of figure 1(g)) if the free kink has the same polarity†) and to the right in the opposite case.

As is seen from figure 1(g), in the former case the kink remains in the pinned state if its shifted position $\xi = \xi_{\min} + \Delta\xi$ lies to the left of the point $\xi = \xi'_{\max}$ conjugate to the potential maximum $\xi_{\max}$, i.e. $|\Delta\xi| \leqslant \xi_{\min} - \xi'_{\max}$. Evidently, $\xi_{\min} - \xi'_{\max} \sim \varepsilon/f$ at $f \leqslant \varepsilon$ (there is no potential well at $f \geqslant \varepsilon$). For $|\Delta\xi|$ the following estimates are valid: in the 'non-relativistic' case $v^2 \ll 1$, i.e. $f^2 \ll \gamma^2$ (see equation (2.16)), $\Delta\xi \approx \log(f^2/\gamma^2)$; in the 'ultrarelativistic' case $1 - v^2 \ll 1$, i.e. $f \geqslant \gamma$, $|\Delta\xi| \simeq 2\sqrt{1 - v^2} \simeq 8\gamma/\pi f$, and we have $|\Delta\xi| \sim 1$ in the intermediate case $(1 - v^2)/v^2 \sim 1$.

To guarantee that the collision does not result in release of the pinned kink, we must demand that $|\Delta\xi| \ll \xi_{\min} - \xi'_{\max}$. This inequality must be investigated separately at $f \sim f_0 \sim \gamma\sqrt{\varepsilon}$ (see equation (2.17)) and at $f \sim \varepsilon$ (see equation (2.5)). Using the above estimates, it is straightforward to conclude that at $f \sim \gamma\sqrt{\varepsilon}$ we need

$$\sqrt{\varepsilon} \log \varepsilon^{-1} \geqslant \gamma$$

while the range $f \sim \varepsilon$ gives rise to a stronger inequality

$$\varepsilon \geqslant \gamma \tag{2.18}$$

which will be assumed to hold (in the SG model) in what follows.

In the case of the kink–antikink collision, when the pinned kink shifts to the right, it will not be released if its shifted position lies to the left of the potential maximum $\xi_{\max}$ (see figure 1(g)). So, in this case, we must demand that $\Delta\xi \ll \xi_{\max} - \xi_{\min}$. Analysis similar to that developed above, but slightly longer, demonstrates that this inequality amounts to $f \geqslant \gamma^{4/3}\varepsilon^{-1/3}$. Inserting $f \sim \varepsilon$ into the latter inequality, we recover the condition (2.18). At the same time, the range $f \sim \gamma\sqrt{\varepsilon}$ gives rise to a more restrictive inequality

$$\varepsilon \geqslant \gamma^{2/5}$$

which will be assumed to hold in the SG model if both polarities are present.

A full analysis of the collision of a free kink with a kink or an antikink pinned by a local potential well will be given elsewhere.

As follows from equations (2.6)–(2.14), of basic interest is the range of voltages $f \sim \varepsilon$. According to the relation (2.18), this implies that $f \geqslant \gamma$. The latter inequality means, according to equation (2.16), that $v(f)$ is close to unity. So equations (2.8)–(2.11), (2.13) and (2.14), together with figures 2 and 3, directly determine the form of the CVC in the range $f \geqslant \varepsilon$.

† In fact, in this case the former free kink becomes pinned, while the former pinned kink is released.

The CVC departs from the dependence $\nu(f)$ in the range $f \lesssim \gamma$ and, as explained above, it terminates at the threshold value (2.17).

Finally, it is important to stress that a full CVC is hysteretic. Indeed, if the DC voltage f increases from zero, one will observe the branch of the CDC described above. However, if f decreases from the values $f \gtrsim \sqrt{M}\varepsilon/\pi$ (i.e. $g \gtrsim 1$; see (2.6)), we shall observe the usual branch of the CVC (2.15), corresponding to $\nu(f) = 1$, up to the terminal value (2.18). The full CVC is shown (for the continuum model (1.7), where the breaks are absent) below in figure 5. If f increases from zero to an intermediate value $f = f_1 \sim \varepsilon$, and then turns back, one will observe an intermediate branch (see broken curve in figure 5) corresponding to $\nu(f) = \nu(f_1)$.

2.2. *The OSG model*

The fundamental difference between this version and the SG model is the fact that, on increase in f, the system remains non-conductive as long as the total density $n_t(f)$ of the kinks which may be in the trapped state is larger than their total density n_0 (Malomed 1989). The quantity $n_t(f)$ can be easily expressed in terms of $\nu(f)$:

$$n_t(f) \simeq l^{-1} \sum_{m=1}^{m_{\max}} \nu(mf) \tag{2.19}$$

where $l^{-1} \ll 1$ is the density of impurities. The terms with $m > 1$ in the sum (2.19) take account of the fact that the impurities for which the value of $U'(\xi)$ at $\xi = \xi_{\inf}$ is equal to $2\pi mf$ or higher can trap m unipolar kinks, the distance between which varies as $\log f^{-1}$. Because of the latter circumstance, the summation in (2.19) must be limited by $m_{\max} \sim l/\log f^{-1}$. Since the maximum value of f at which the impurities can detain the kinks is $f_{\max} = \sqrt{M}\varepsilon/\pi$ (which corresponds to $g = 1$; see (2.6)), in the range $f_{\max}/2 < f < f_{\max}$ there remains the single term with $m = 1$. The dependence $n_t(f)$ has breaks at the values $f = f_{\max}/m$, and less conspicuous breaks at $f = f_{1,2}/m$, where $f_{1,2} < f_{\max}$ are the values marked by arrows in figures 2 and 3, at which the dependence $\nu(f)$ demonstrates breaks. So, the system is not conductive at f such that $n_0 < n_t(f)$ (the case $n_0 > n_t(0)$ is excluded by the underlying assumption $n_0 \ll 1$), and in the range where $n_0 > n_t(f)$ its CVC is given by equation (2.15). The velocity of a free kink in the OSG model is

$$v(f) = \pi f/4\bar{\gamma} \tag{2.20}$$

(cf equation (2.16)).

It is necessary to note that the solitonic conductivity of the OSG model is of the relay type; when a moving kink encounters a unipolar trapped kink (or a cluster of trapped kinks), it stops and becomes trapped, while one of the formerly trapped kinks becomes free. In fact, the same pertains to the SG model when unipolar kinks collide (under the condition (2.17)).

The aforementioned particular case $n_0 \ll l^{-1}$ (one kink per many impurities) deserves special attention. In this case the value $f = f_0$ at which $n_t(f) = n_0$ is close to $f_{\max}$ where

$$(f_{\max} - f_0) f_{\max}^{-1} \sim (n_0 l)^2 \ll 1 \tag{2.21}$$

and the CVC takes the form shown in figure 4. This CVC is not hysteretic, unlike that of the SG model.

3. The continuum model

Our analysis of the models (1.2) and (1.5) with the right-hand side (1.7) is based on the well known expression for the probability-density functional of the Gaussian random fields:

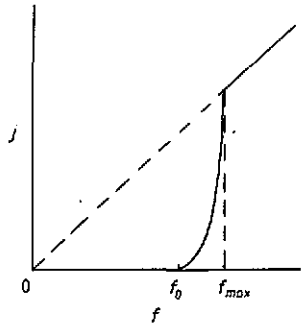

Figure 4. The CVC (I–V characteristic) (2.15) of the overdamped SG model (1.5) in the case $n_0 \ll I^{-1} \ll 1$. The broken straight line corresponds to $\nu(f) \equiv 1$.

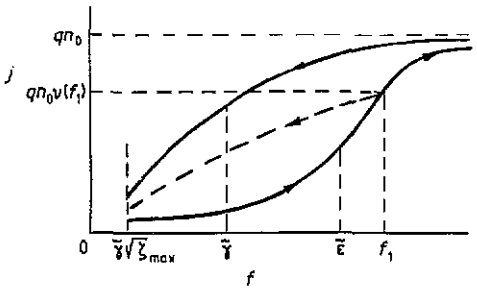

Figure 5. The hysteretic CVC (I–V characteristic) of the SG continuum models (1.2) and (1.7). The arrows indicate the sense of the particular branches of the CVC.

$$P\{\xi_1(x), \xi_2(x)\} \sim \exp[-(2\bar{\varepsilon}^2)^{-1} \int_{-\infty}^{+\infty} dx\, [\xi_1^2(x) + \xi_2^2(x)]. \tag{3.1}$$

An effective one-kink potential corresponding to the right-hand side (1.7) of equations (1.2) and (1.5) is (cf (2.1))

$$U(\xi) = \int_{-\infty}^{+\infty} dx \sum_{p=1,2} \zeta_p(x) U_p(\xi - x) \tag{3.2}$$

where

$$U_1(z) \equiv M\{1 + \cos[M^{-1}\varphi_k(z)]\} \qquad U_2(z) \equiv M\{1 - \sin[M^{-1}\varphi_k(z)]\} \tag{3.3}$$

φ_k being the kink's waveform (1.3).

The required quantity $\nu(f)$ is determined by a probability distribution $p(f)$ of the values $f_{inf} \equiv (1/2\pi)U'(\xi_{inf})$ at the inflection points $\xi_{inf}(U''(\xi_{inf}) = 0)$. Straightforward calculation of a corresponding Gaussian continual integral yields

$$p(f_{inf}) = 2(2\pi/I_1)^{1/2}\varepsilon^{-1} \exp(-2\pi^2 f_{inf}^2/I_1\varepsilon^2) \tag{3.4}$$

where

$$I_j \equiv \int_{-\infty}^{+\infty} dx \sum_{p=1,2} \left(\frac{d^j U(x)}{dx^j}\right)^2 \tag{3.5}$$

(besides I_1, we shall also need I_2 and I_3). It is evident that

$$\nu(f) = \int_0^f p(f_{inf})\, df_{cf} = \mathrm{erf}(\sqrt{2}\pi f/\sqrt{I_1}\varepsilon) \tag{3.6}$$

where

$$\mathrm{erf}(z) \equiv 2\pi^{-1/2} \int_0^z \exp(-t^2)\, dt.$$

3.1. The SG model

In the SG version of the continuum model, insertion of equations (3.6) and (2.16) into (2.15) yields the CVC shown in figure 5. As was explained in the preceding paragraph,

this CVC is hysteretic. As in the discrete model, we need the condition $\varepsilon \gg \gamma$ in the case of unipolar kinks, and $\varepsilon \gg \gamma^{2/5}$ in the opposite case to guarantee that collisions between free and trapped kinks do not change $\nu(f)$. Note that, from the viewpoint of equation (3.6), the range $f \sim \varepsilon$ is of basic interest. Because of the conditions mentioned, in this range $f \gg \gamma$, so that $\nu(f)$ is close to unity, and the form of the CDC coincides with the dependence (3.6). Finally, it is noteworthy that the CDC of the continuum SG model, unlike the CVC of the discrete model, demonstrates no breaks. One may regard the continuum-model CVC as a 'smoothed version' of the discrete-model CVC.

We mentioned above that free kinks can be trapped again by local potential barriers. To avoid this effect, it is necessary to demand that the values taken by the random functions $\zeta_{1,2}(x)$ be limited by some $\zeta_{\max}$ such that $\gamma^2\zeta_{\max} \ll \varepsilon^2$. Strictly speaking, the limited random functions cannot be Gaussian. However, it is easy to see that, owing to the assumed inequality $\varepsilon \gg \gamma$, the limitation is not significant. For small f, the CVC terminates at the threshold value $f = f_0 \sim \gamma\sqrt{\zeta_{\max}} \ll \varepsilon$ (cf (2.18)).

3.2. The OSG model

In the OSG version of the continuum model, the central point is to find the maximum density $n_t(f)$ of the kinks which can be detained in a trapped state at a given f. This density is proportional to the mean density $\bar{l}^{-1}$ of the inflection points $\xi_{\inf}$. Using standard methods (see, e.g., section 3.4 of the book by Ziman (1979)), one can find that $\bar{l}^{-1} = \pi^{-1}(I_3/I_2)^{1/2}$, $I_{2,3}$ being defined in (3.5). Evidently, $\bar{l}$ is of order unity, in contrast with the discrete model where we assumed that $l \gg 1$.

As above, the system becomes conductive at $f = f_0$ such that $n_t(f_0) = n_0$. Because of the underlying assumption $n_0 \ll 1$, it is necessary that $1 - \nu(f_0) \sim n_0 \ll 1$, i.e. $f_0 \gg \varepsilon$. Using equation (3.6), it is easy to find that

$$f_0^2 \simeq (I_1/2\pi^2)\varepsilon^2 \log n_0^{-1} \tag{3.7}$$

(to simplify equation (3.7), we have strengthened the assumption $n_0 \ll 1$ to $\log n_0^{-1} \gg 1$). In the range $f \gtrsim f_0$, many-kink contributions to $n_t(f)$ may be neglected, and it takes the form

$$n_t(f) \simeq l_0^{-1}\nu(f) \simeq \pi^{-5/2}(I_1 I_3/I_2^2)^{1/2}\varepsilon f^{-1} \exp(-2\pi^2 f^2/I_1\varepsilon^2). \tag{3.8}$$

So, insertion of equations (3.8) and (2.20) into equation (2.15) yields the CVC of the continuum OSG model:

$$j \simeq qn_0(\pi f/4\tilde{\gamma})\{1 - \exp[-(4\pi^2 f_0/I_1\varepsilon^2)(f - f_0)]\} \tag{3.9}$$

f_0 being defined in (3.7). The CVC (3.9) is qualitatively similar to that shown in figure 4. However, there is no sharp break at $f = f_{\max}$, and the size of the transient range is (cf (2.21))

$$(f_{\max} - f_0)f_0^{-1} \sim 1/\log n_0^{-1}. \tag{3.10}$$

Thus, we can again infer that, proceeding from the discrete model to the continuum model, we obtain a similar CVC but in a smoothed form.

3.3. Additional comments

As we mentioned in section 1, equation (1.2) with the right-hand side (1.7), where $M = 1$ and $\zeta_2 = 0$, coincides with the model of a damped randomly inhomogeneous

driven LJJ proposed by Mineev *et al* (1981). The only difference is that in the LJJ theory the quantities $v(f)[n_0 - n_t(f)]$ and f have the opposite meanings to those in the CDW theory; the former is proportional to the DC voltage across the junction, while the latter is the density of the DC bias current. As to the kink (1.3), it represents a fluxon, i.e. a magnetic flux quantum. The overdamped model (1.5) describes a driven LJJ of SNS type: two bulk superconductors separated by a thin layer of a normal metal. In a real LJJ, an important role may also belong to random inhomogeneities of the junction's inductance (Sakai *et al* 1987) and capacity (Malomed and Ustinov 1990). They are accounted for by the additional terms

$$[\zeta_3(x)]_x \varphi_x + \zeta_4(x)\varphi_{tt} \tag{3.11}$$

in the right-hand side (1.7) of equation (1.2) (with $M = 1$, $\zeta_2 = 0$). Here $\zeta_{3,4}(x)$ are Gaussian random functions subject to correlations (1.8) and (1.9) with $\tilde{\varepsilon}$ replaced by some $\tilde{\varepsilon}_3$ and $\tilde{\varepsilon}_4$. All the equations (3.4)–(3.10) are directly applicable to this variant of the continuum model, with the modification that in equation (3.2) the summation index p takes two values 1 and 3, where $U_3(x) \equiv -4(\tilde{\varepsilon}_3/\tilde{\varepsilon})\,\mathrm{sech}^2 x$.

It is also natural to consider a discrete model of a randomly inhomogeneous LJJ based on the equation (cf equation (1.2))

$$\varphi_{tt} + \gamma\varphi_t - \varphi_{xx} + \sin\varphi + f = \sum_n \varepsilon_n \sin\varphi\ \delta(x - x_n) \tag{3.12}$$

where $l \gg 1$ and the parameters ε_n are subject to the Gaussian distribution (cf (3.4))

$$p(\varepsilon_n) = (\sqrt{\pi}\tilde{\varepsilon})^{-1} \exp(-\varepsilon_n^2/\tilde{\varepsilon}^2). \tag{3.13}$$

The model described by equations (3.12) and (3.13) can be realized in an experiment as a LJJ with a random lattice of the so-called micro-resistors ($\varepsilon_n > 0$) and micro-shorts ($\varepsilon_n < 0$), i.e. local defects where tunnelling of the superconducting electrons across the dielectric barrier is, respectively, suppressed ($\varepsilon_n > 0$) or enhanced ($\varepsilon_n < 0$). Investigation of the model (3.12) and (3.13) yields results which are the same as those obtained in the framework of the corresponding continuum model.

It is noteworthy that the models (1.2) and (1.5) with the terms (1.7) and (3.11) on the right-hand sides are applicable, with slight modifications, to a number of other physical objects. Examples are disordered quasi-one-dimensional ferromagnets (Kivshar *et al* 1986), and an atomic-chain continuum model of the Frenkel–Kontorova type with a substrate potential containing a randomly modulated component.

To conclude this section, let us make one more comment concerning the CDW system. To observe the CVCs derived in the preceding and present sections, it is necessary to include a CDW conductor in a closed electric circuit. Our analysis assumed tacitly that the conversion of the charged solitons into conductivity electrons, and vice versa, at junction points between the CDW conductor and metallic conductors did not change the total number of solitons (a microscopic model of the conversion was put forward by Krive *et al* (1987)); in principle, one may also consider a closed ring-like CDW conductor (cf a ring-like LJJ realized in the experiment of Davidson *et al* (1985)), in which the driving DC voltage is induced by a vortex electric field.

The soliton number conservation can be readily realized in a LJJ of a finite length; if an external magnetic field is absent, the corresponding perturbed SG equation must be supplemented by the boundary conditions $\varphi_x = 0$ at the junction edges (see, e.g., the book by Barone and Paterno (1982)). Because of these conditions, a moving soliton (fluxon) will be reflected by an edge in the form of an antifluxon. This effect is the basis

for explanation of the so-called zero-field steps on a junction's CVC as a manifestation of fluxon oscillations between the reflecting edges (Fulton and Dynes 1973).

4. Radiative effects

If the dissipation constant γ in the SG model (1.2) is sufficiently small, radiative losses in the form of emission of quasi-linear waves may essentially affect the kink's law of motion, i.e. the form of the CVC. We shall analyse the radiative losses by means of the perturbation theory for SG solitons based on the inverse scattering transform (IST). A variant of this theory suitable for the emission problems has been given in detail by Malomed (1987a, b). In terms of the IST technique (Zakharov *et al* 1980), a radiative component of the SG wave field is described by an amplitude $B(k)$, k being the radiation wavenumber. The spectral density of the radiation energy E can be expressed in terms of $B(k)$ as follows:

$$\mathcal{E}(k) \equiv \mathrm{d}E/\mathrm{d}k = (4/\pi)\,|B(k)|^2 + \mathrm{O}(|B(k)|^4). \tag{4.1}$$

The IST-based perturbation theory rests upon the perturbation-induced evolution equation for $B(k)$ derived by Kaup and Newell (1978) and others. For one kink, this equation can be represented in the following form (Malomed 1987a, b):

$$\frac{\mathrm{d}B(k)}{\mathrm{d}t} = -\frac{i\tilde{\varepsilon}}{4}(\lambda^2 + \nu^2)^{-1}\int_{-\infty}^{+\infty} \mathrm{d}x\, P[\varphi_k(z)](\lambda^2 - \nu^2 - 2i\nu\lambda \tanh z)\exp(-ikx + i\omega t) \tag{4.2}$$

where $\nu^2 \equiv \frac{1}{2}(1+v)(1-v)^{-1}$, $\lambda \equiv \frac{1}{2}(k+\omega)$, $\omega \equiv (k^2+1)^{1/2}$, $z \equiv (x-vt)(1-v^2)^{-1/2}$, $\varphi_k(z)$ is the kink's waveform (1.3) and $\tilde{\varepsilon}P[\varphi]$ is an emission-generating perturbation in the right-hand side of the SG equation.† The further analysis is in principle different for the discrete and continuum models, although eventual results prove to be quite similar.

4.1. The discrete model

In the case $l \gg 1$ (recall that l is the mean distance between the impurities), the first step is to calculate the energy E emitted by a kink colliding with an isolated impurity. For the case $M = 1$ this problem has been solved by one of the authors (Malomed 1988). The general idea is evident; assuming that $B(k) = 0$ at $t = -\infty$ (prior to the collision), calculate the final value

$$B_f(k) \equiv B(k, t = +\infty) = \int_{-\infty}^{+\infty} \frac{\mathrm{d}B(k)}{\mathrm{d}t}\,\mathrm{d}t. \tag{4.3}$$

Next, insert the value (4.3) into equation (4.1), and calculate the total emitted energy

$$E(v) \equiv \int_{-\infty}^{+\infty} \mathcal{E}(k)\,\mathrm{d}k. \tag{4.4}$$

The total energy (4.4) can be found in an analytical form in two limiting cases: $v^2 \ll 1$ and $1 - v^2 \ll 1$. In the former case,

$$E(v) \sim \exp(-\pi/v) \tag{4.5}$$

if $\varepsilon \ll v^2 \ll 1$ (Mineev *et al* 1981), and $E \sim \exp(-c/\sqrt{\varepsilon})$ with $c \sim 1$, if $v^2 \ll \varepsilon$ (Malomed

† The amplitude $B(k)$ is related to $b(\lambda)$ defined by Zakharov *et al* (1980) as follows: $B(k) \equiv b(\lambda)\exp(i\omega t)$.

1985, 1988). These estimates are valid irrespective of the value of the commensurability index M.

In the latter case ($1 - v^2 \ll 1$), which is of the most interest, realization of the outlined programme for calculation of $E(v)$ encounters a difficulty. We shall explain it in detail for $M = 2$. Substitution of the right-hand side of equation (1.2) into equation (4.2) yields a term

$$(\varepsilon/4) \sin \theta_n \, (\lambda^2 + \nu^2)^{-1}\{\lambda^2 - \nu^2 + 2i\nu\lambda \tanh[vt(1 - v^2)^{-1/2}]\}$$
$$\times \tanh[vt(1 - v^2)^{-1/2}] \exp(i\omega t). \tag{4.6}$$

Insertion of the term (4.6) into equation (4.3) gives rise to a divergence. This divergence is of a rather general nature, and a general way to circumvent it is as follows (Malomed 1987a, b): insert $\varphi(x, t)$ into equation (4.2) in the form

$$\varphi(x, t) = \varphi^{(0)}(x) + \varphi_R(x, t) \tag{4.7}$$

where the background field $\varphi^{(0)}(x)$ is a solution of the linearized version of equation (1.2) far from the kink (at $|x| \to \infty$). A resultant SG equation for the *renormalized* wave field $\varphi_R(x, t)$ contains a new *renormalized* perturbation P_R which gives rise to no divergence. In particular, for $M = 2$,

$$\varphi^{(0)}(x) = (\tilde{\varepsilon}/2) \sin \theta_n \exp(-|x - x_n|) \operatorname{sgn} t \tag{4.8}$$

$$\tilde{\varepsilon} P_R = \tilde{\varepsilon} \cos \theta_n \sin \varphi_R \, \delta(x - x_n) + 2\varphi^{(0)} \sin^2 \varphi_R$$
$$+ \tilde{\varepsilon} \sin \theta_n \, \delta(x - x_n)(\cos \varphi_R - \operatorname{sgn} t)$$
$$- \tilde{\varepsilon} \sin \theta_n \exp(-|x - x_n|)\delta'(t) + O(\tilde{\varepsilon}^2) \tag{4.9}$$

(recall that we are considering an isolated impurity, and that $\tilde{\varepsilon} \equiv \sqrt{M}\varepsilon$; see equation (1.2)). The multiplier $\operatorname{sgn} t$ in equation (4.8) (it gives rise to the term $\sim\delta'(t)$ in equation (4.9)) arises because $\cos[\varphi_k(t \to \pm\infty)] = \operatorname{sgn} t$ (for definiteness, we set $\sigma = +1$ in equation (1.3)).

Calculations with the perturbation (4.9) prove to be extremely tedious. In the case $M > 2$, when not only $\cos \varphi_k$ but also $\sin \varphi_k$ takes different limiting values at $t \to \pm\infty$, the renormalized perturbation and calculations based on it are still more laborious. However, there is a less rigorous but much simpler approach. Indeed, let the evolution equation (4.2) have the form

$$dB(k)/dt = F(k, t) \exp(i\omega t) \tag{4.10}$$

where the function $F(k, t)$ takes different limiting values at $t \to \pm\infty$ (cf (4.6)). We seek a solution to equation (4.10) in the form

$$B(k, t) = -(i/\omega)F(k, t) \exp(i\omega t) + B_R(k, t) \tag{4.11}$$

where $B_R(k, t)$ is governed by the equation

$$dB_R(k)/dt = -(i/\omega)[dF(k, t)/dt] \exp(i\omega t). \tag{4.12}$$

While the quantity $B_f(k)$ defined according to (4.3) is divergent, the analogous quantity $[B_f(k)]_R$, defined by inserting equation (4.12) into (4.3), is convergent. Note that replacing $B_f(k)$ by the renormalized $[B_f(k)]_R$ is equivalent to integration by parts in (4.3). The meaning of this simplified version of the renormalization procedure is that $B_R(k)$ represents the amplitude of the emitted radiation proper, while the first term in (4.11)

describes a non-radiation background field equivalent to $\varphi^{(0)}(x)$ in (4.7). It is easy to see that interference between the two terms gives no actual contribution to the emitted energy when the sum (4.11) is inserted into equation (4.1). In this way, we obtain for $M = 2$ the following emitted energy spectral density (we assume that $v^2 \gg \varepsilon$, but the inequality $1 - v^2 \ll 1$ is not required):

$$\mathcal{E}(k) = (\pi\tilde{\varepsilon}^2/4)v^{-4}(1 - v^2) \times [\![\sin^2\theta_n \cosh^2\{\pi[(1 + k^2)(1 - v^2)]^{1/2}/2v\} + \cos^2\theta_n \operatorname{sech}^2\{\pi[(1 + k^2)(1 - v^2)]^{1/2}/2v\}]\!]. \tag{4.13}$$

In the limit $v^2 \ll 1$, the corresponding total emitted energy (4.4) is exponentially small in accordance with (4.5). In the opposite limit $1 - v^2 \ll 1$,

$$E \simeq \tilde{\varepsilon}^2 \sin^2\theta_n \tag{4.14}$$

does not vanish, in contrast with the case $M = 1$, where $E = \frac{8}{3}\varepsilon^2(1 + \sin^2\theta_n)(1 - v^2)^{1/2}$ (Malomed 1988). The limiting forms of $\mathcal{E}(k)$ and E for $1 - v^2 \to 0$ can also be found for arbitrary $M \geqslant 2$:

$$\mathcal{E}(k) = \pi^{-1}\tilde{\varepsilon}^2(1 + k^2)^{-1} \sin^2(\pi/M) \cos^2(\theta_n + \pi/M + 2\pi m/M) \tag{4.15}$$

$$E = \tilde{\varepsilon}^2 \sin^2(\pi/M) \cos^2(\theta_n + \pi/M + 2\pi m/M). \tag{4.16}$$

The additional integer m in these expressions indicates that we may add $2\pi m$ to the kink's waveform (1.3). Evidently, in the case $M = 2$, (4.15) coincides with the limiting form of (4.13), and (4.16) is equivalent to (4.14). Note that (4.15) and (4.16) become zero at $M = 1$, in accordance with the above.

The kink's law of motion is determined by the energy balance equation

$$2\pi f v = 8\tilde{\gamma}v^2(1 - v^2)^{-1/2} + W(v) \tag{4.17}$$

where the first term on the right-hand side gives the rate of dissipative energy losses, and the second term is the energy emission rate

$$W(v) = l^{-1}v\langle E(v)\rangle \tag{4.18}$$

the angular brackets indicating averaging in the phase θ_n (Malomed 1988). It is important whether the dependence $W(v)$ is monotonic. In the case $M = 1$ it is non-monotonic, which gives rise to a radiative hysteresis in the range

$$(8/\pi^2)\varepsilon^2\gamma/l \leqslant (2\pi f)^2 \leqslant (\varepsilon^2/l)^2 \tag{4.19}$$

provided that

$$8\gamma l \ll \varepsilon^2 \tag{4.20}$$

(Malomed 1988). The dependences of the quantity $vE(v)$ on v are shown for $M = 2$ and different values of θ_n in figure 6. Evidently, averaging in θ_n is equivalent to setting $\theta_n = \pi/4$. As is seen from figure 6, at $\theta_n = \pi/4$ the dependence is not hysteretic, so that the radiative hysteresis does not take place at $M = 2$; it seems very similar that at $M > 2$ it does not take place either. Nevertheless, under the same condition (4.20) the emission-affected CVC for $M \geqslant 2$ differs significantly from the usual one in the range $8\gamma \leqslant 2\pi f \leqslant$

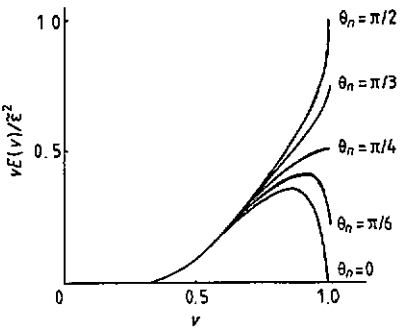

Figure 6. The dependences of $vE(v)/\tilde{\varepsilon}^2$ on v for $M = 2$ and different values of θ_n. On increase in θ_n, the dependence ceases to be non-monotonic at $\theta_n = \pi/4$.

ε^2/l (cf (4.19)) (figure 7). Note that these values of f are much smaller than $f \sim \varepsilon$ at which the hysteresis studied in section 2 (figure 5) takes place.

4.2. The continuum model

If emission of radiation is generated by the perturbing term (1.7), it is natural to define the spectral density $\mathcal{W}(k)$ of the energy emission rate W. According to equation (4.1),

$$\mathcal{W}(k) \equiv dW/dk \equiv (d/dt)[\mathcal{E}(k)] = 8\pi \operatorname{Re}[B(k)\, dB^*(k)/dt] \tag{4.21}$$

where Re and * represent the real part and complex conjugation, respectively. According to the papers of Malomed (1984, 1987a, b), the quantity $B(k)$ in equation (4.21) can be obtained by integrating equation (4.2) in time, in the limits $-\infty < t' < t$, with the use of a formal trick; the right-hand side of (4.2) must be multiplied by $\exp(\mu t)$ with an infinitely small $\mu > 0$. The trick implies adiabatically turning on the emission process 'turned off' at $t = -\infty$. After the integration, μ must be set equal to zero with regard to the known relation

$$\lim_{\mu \to 0} (i\chi + \mu)^{-1} = P(1/i\chi) - i\delta(\chi) \tag{4.22}$$

P being the symbol for the principal value (when the expression (4.22) is inserted into an integral). Straightforward calculations which can be performed in a general form, yield the following result:

$$\mathcal{W}(k) = 2v\langle \mathcal{E}(k) \rangle \tag{4.23}$$

$$W \equiv \int_{-\infty}^{+\infty} \mathcal{W}(k)\, dk = 2v\langle E(v) \rangle \tag{4.24}$$

(cf (4.18)), where $\langle \mathcal{E} \rangle$ and $\langle E \rangle$ are the spectral density and the total emitted energy for an isolated impurity averaged in θ_n (see above). The parameter $\tilde{\varepsilon}$ in the corresponding expressions for $\langle \mathcal{E} \rangle$ and $\langle E \rangle$ (see, e.g., (4.13)–(4.16)) must be taken to be the same as in equation (1.9). So, the radiative effects in the continuum model are quite similar to those in the discrete model. In particular, at $M = 1$, substitution of the expression $\langle E(v) \rangle \simeq \tilde{\varepsilon}^2(1 - v^2)^{1/2}$ for $1 - v^2 \ll 1$, taken from the paper of Malomed (1988), into equation (4.24) yields

$$W \simeq 2\tilde{\varepsilon}^2(1 - v^2)^{1/2}. \tag{4.25}$$

In this case ($M = 1$), radiative hysteresis may take place. As follows from a comparison

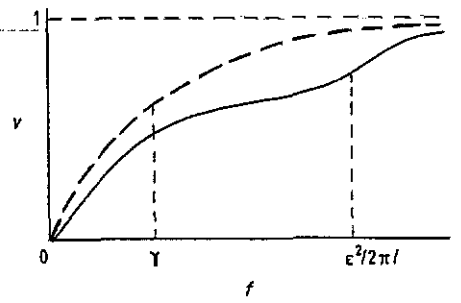

Figure 7. The emission-affected dependence $v(f)$ for $M = 2$ under the condition (4.20). The broken curve corresponds to the usual dependence (2.16).

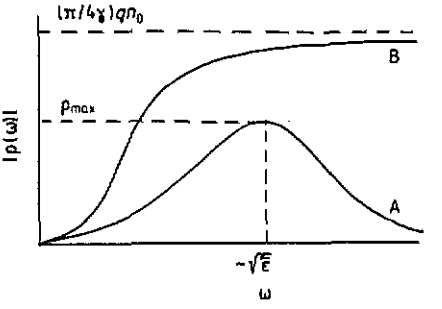

Figure 8. Dependence of the AC conductivity $|\rho(\omega)|$ on the AC frequency ω in the continuum model: curve A, SG version; curve B, OSG version.

of equations (4.18) and (4.24), we should set $l \sim 1$ in the corresponding estimates (4.19) and (4.20) for the continuum model. It follows from (4.19) (with $l \sim 1$) that the radiative hysteresis and the hysteresis in the range $f \sim \varepsilon$ revealed in section 3 must be easily distinguishable.

To conclude the present section, let us briefly discuss radiative effects in LJJs described by continuum models similar to (1.2) and (1.7). As we mentioned above, the simplest model of this kind is that with $M = 1$, $\zeta_2(x) \equiv 0$. In the limit $1 - v^2 \to 0$, the energy emission rate in this model differs by the multiplier $\frac{1}{3}$ from equation (4.25). The radiative hysteresis in this model has been revealed by Mineev *et al* (1981). If the inductance and capacity inhomogeneities described by the additional perturbing terms (3.11) are taken into account, the expression for W at $1 - v^2 \ll 1$ changes drastically (see also the paper by Malomed and Ustinov (1990)):

$$W \simeq \tfrac{2}{3}(4\tilde{\varepsilon}_3^2 + \tilde{\varepsilon}_4^2)(1 - v^2)^{-3/2}. \tag{4.26}$$

Insertion of this into equation (4.17) leads to the asymptotic law of motion

$$1 - v^2 \simeq [(4\tilde{\varepsilon}_3^2 + \tilde{\varepsilon}_4^2)/3\pi f]^{2/3} \tag{4.27}$$

instead of $1 - v^2 \simeq (4\gamma/\pi f)^2$ ensuing from equation (2.16). It is necessary to note that the additional dissipative term $-\beta\varphi_{txx}$ (with positive β), which, generally speaking, should be added to the left-hand side of equation (1.2), gives rise to a rate of energy losses also proportional to $(1 - v^2)^{-3/2}$ (cf (4.26)). This dissipative term plays a significant role in the theory of LJJs (see, e.g., Olsen and Samuelsen 1984). Of course, the consideration of the 'ultrarelativistic' kinks ($1 - v^2 \ll 1$) in the framework of the CDW theory is meaningful as long as the 'Lorenz-contracted' kink's size $\sim(1 - v^2)^{1/2}$ remains greater than the spacing of the underlying lattice.

5. AC conductivity

Let us proceed to the case when the system is subject to the action of the AC field (1.10) with a sufficiently small amplitude F. If a kink was located at a local minimum ξ_0 of an

effective potential $U(\xi)$, under the action of the AC drive it performs small oscillations described, in complex notation, by the equation

$$\ddot{\xi} + \bar{\gamma}\dot{\xi} + \kappa(\xi - \xi_0) = (\pi/4)F\exp(i\omega t) \tag{5.1}$$

where

$$\kappa \equiv \tfrac{1}{8}U''(\xi_0) \tag{5.2}$$

(recall that $\bar{\gamma} \equiv M^{-1/2}\gamma$; see equation (1.2)). Equation (5.1) pertains to the SG model; in the case of the OSG model, the term $\ddot{\xi}$ must be dropped.

A solution to equation (5.1) is

$$\xi = \sigma(\omega)F\exp(i\omega t) \qquad \sigma(\omega) \equiv (\pi/4)(\kappa^2 - \omega^2 + i\bar{\gamma}\omega)^{-1}. \tag{5.3}$$

A corresponding contribution to the AC current is (cf equation (2.15))

$$q\dot{\xi} = iq\omega\sigma(\omega)F\exp(i\omega t).$$

Proceeding from this expression, it is natural to define the AC conductivity (Malomed 1988) as

$$\rho(\omega) \equiv iqn_0\omega\langle\sigma(\omega)\rangle \tag{5.4}$$

where $\langle \ldots \rangle$ indicates averaging in a disordered potential and, as above, n_0 is the total density of the kinks. Further analysis is different for the discrete and continuum models.

5.1. The discrete model

Let us denote by p_M the probability for a kink to reside in a potential well (figure 1(*b*) or 1(*c*)) in the absence of an external drive. In the version of the discrete model which corresponds to equations (2.8) and (2.9), i.e. neglects tunnelling under the potential humps (figure 1(*e*) and 1(*f*)), $p_M = M^{-1}(M+1)^{-1}(3M-1)$. In the alternative version (corresponding to equations (2.13) and (2.14)), $p_M = \frac{1}{2}M^{-2}(M+1)^{-1}(3M+1)(2M-1)$. If the kink resides in a well, it is easy to find the quantity (5.2):

$$\kappa = \tfrac{1}{2}M^{-1/2}\varepsilon\sin^2[(M/2)(\pi - \theta_n)] \tag{5.5}$$

where θ_n varies within the interval $\pi - 2\pi/M < \theta_n < \pi$. If the kink resides in a wide valley between two potential steps, the corresponding probability being $1 - p_M$, we may set $\kappa = 0$. So, applying averaging in θ_n to equations (5.3)–(5.5), we find that

$$\rho(\omega) = -(i\pi/4)qn_0\omega\{(1-p_M)(\omega^2 - i\bar{\gamma}\omega)^{-1} \times p_M[(\omega^2 - i\bar{\gamma}\omega)(\omega^2 - \varepsilon/2\sqrt{M} - i\bar{\gamma}\omega)]^{-1/2}\}. \tag{5.6}$$

In the limit $M \to \infty$ the probability p_M vanishes, and equation (5.6) turns into the AC conductivity of the homogeneous system: $\rho_0(\omega) = -(i\pi/4)qn_0\omega(\omega^2 - \kappa^2 - i\bar{\gamma}\omega)^{-1}$. In the case of the OSG model, the difference reduces to dropping the term ω^2 in equation (5.6).

Setting $\tilde{\gamma} = 0$ in (5.3) and (5.6), we see that the averaging in θ_n transforms the resonant pole singularity of $\sigma(\omega)$ at $\omega^2 = \kappa^2$ into the weaker root singularity of $\rho(\omega)$ at $\omega^2 = \varepsilon/2\sqrt{M}$. The same effect has been noted by Malomed (1988) for $M = 1$.

5.2. The continuum model

Proceeding from the fundamental probability-density functional (3.1), it is straightforward to find the probability distribution of the values κ:

$$p(\kappa) = 2(2\pi I_2)^{-1/2}\varepsilon^{-1}\exp(-\kappa^2/2I_2\varepsilon^2) \tag{5.7}$$

(cf (3.4)), where I_2 is defined by (3.5). The averaging of equations (5.4) and (5.3) in κ on the basis of the probability distribution (5.7) can be represented in an explicit form in two limiting cases: $\omega^2 \ll \varepsilon$ and $\omega^2 \gg \varepsilon$. In the former case,

$$|\rho(\omega)| \simeq (2\pi/I_2)^{1/2}(qn_0\omega/\tilde{\varepsilon})\log[\tilde{\varepsilon}^2/\omega^2(\tilde{\gamma}^2 + \omega^2)] \tag{5.8}$$

(we treat the logarithm in (5.8) as a large quantity).

In the latter case, $|\rho(\omega)| \simeq (\pi/4)qn_0\omega^{-1}$ (which is the AC conductivity of the homogeneous system). The full dependence $|\rho(\omega)|$ for the continuum model is depicted schematically by curve a in figure 8. A maximum value $\rho_{\max} \sim qn_0\tilde{\varepsilon}^{-1/2}$ is attained at $\omega \sim \sqrt{\tilde{\varepsilon}}$. It is noteworthy that, in the continuum model, the dependence $\rho(\omega)$, demonstrates no trace of a resonant singularity at $\omega^2 \sim \tilde{\varepsilon}$, unlike the dependence (5.6) for the discrete model. This is another manifestation of the trend noted above in the DC case; proceeding to the continuous model exerts a 'smoothing' effect on the characteristics of the system.

In the overdamped version of the continuum model, we obtain the following expressions: $|\rho(\omega)| \simeq (2\pi/I_2)^{1/2}(qn_0\omega/\tilde{\varepsilon})\log[\tilde{\varepsilon}^2/(\omega\tilde{\gamma})^2]$ at $\omega\tilde{\gamma} \ll \tilde{\varepsilon}$, and $|\rho(\omega)| \simeq (\pi/4\tilde{\gamma})qn_0$ at $\omega\tilde{\gamma} \gg \tilde{\varepsilon}$, the latter expression being that for the homogeneous system. The full dependence $|\rho(\omega)|$ is depicted by curve B in figure 8.

In conclusion, it is relevant to note that in our model the contribution of the continuous spectrum to the solitonic AC conductivity is negligible, in contrast with the model of a homogeneous overdamped system studied by Horovitz and Trullinger (1984).

6. Conclusion

The results of this paper, as well as those obtained by Malomed (1988, 1989), lead to the following inference: the general consequences of the idea that kinks trapped initially by an effective disordered potential escape gradually on increase in the DC drive or oscillate under the action of AC drive are more or less insensitive to details of the model.

To conclude the paper, let us briefly discuss the possibility of experimental verification of the principal predictions obtained in the framework of the present model. First of all, both versions of the model (SG and OSG) demonstrate a conductivity threshold, the threshold voltage being much larger in the OSG model (see figure 4). The standard (Maki's) model of the solitonic conductivity also demonstrates a threshold, but its nature is altogether different. A noticeable feature of our OSG model is the dependence of the threshold voltage f_0 on the density l^{-1} of the charged impurities, given by equation (3.7):

$$f_0^2 \sim \tilde{\varepsilon}^2/\log(n_0^{-1}) \sim l^{-1}/\log(n_0^{-1}) \tag{6.1}$$

(recall that the renormalized coupling constant $\tilde{\varepsilon}^2$ in equation (1.9) includes the multi-

plier l^{-1}, l being the mean distance between the charged impurities; equation (6.1) pertains to the realistic case $l \ll 1$). In principle, the impurity density l^{-1} may be experimentally controllable by doping the system, which opens the way to verify the relation (6.1).

The fact that the maximum conductivity in our model is proportional to the total density n_0 of the kinks (which is assumed to be conserved) can also be amenable to an experimental test, since the density may depend on an initial state of a sample. Note, however, that the threshold voltage contains only a weak logarithmic dependence on n_0 according to equation (6.1).

Finally, one may try to relate the strongly pronounced hysteretic behaviour of the CVC, predicted by the SG version of our model, to hystereses sometimes observed in experiments with CDW systems. However, this version of the model may only be applied to systems with weak dissipation, which is difficult to realize in real CDW conductors.

We defer a minute comparison of our results with available experimental data to another paper. A complicating role may be played by the fact that, in real near-commensurate systems, different mechanisms, e.g. Maki's and ours, may simultaneously contribute to the solitonic conductivity.

Acknowledgments

One of the authors (BAM) is indebted to I V Krive, A S Rozhavsky and A F Volkov for useful discussions of the problems considered in the present paper.

References

Apostol M and Baldea I 1985 *Solid State Commun.* **53** 687
Barnes S E and Zawadowski A 1983 *Phys. Rev. Lett.* **51** 1003
Barone A and Paterno G 1982 *Physics and Applications of the Josephson Effects* (New York: Wiley)
Davidson A, Dueholm B, Krygger B and Pedersen N F 1985 *Phys. Rev. Lett.* **55** 2059
Dueholm B, Joergensen E, Pedersen N F, Samuelsen M R, Olsen O H and Cirillo M 1981 *Physica* B **108** 1303
Efetov K B and Larkin A I 1977 *Zh. Eksp. Teor. Fiz.* **72** 2350
Erne S N and Ferrigno A 1983 *Phys. Rev.* B **27** 5440
Fogel M B, Trullinger S E, Bishop A R and Krumhansl A 1976 *Phys. Rev. Lett.* **36** 1411
Fukuyama H 1978a *J. Phys. Soc. Japan* **45** 474
—— 1978b *J. Phys. Soc. Japan* **45** 1266
Fukuyama H and Lee P A 1978 *Phys. Rev.* B **17** 535
Fulton T A and Dynes R C 1973 *Solid State Commun.* **12** 57
Grüner G 1988 *Rev. Mod. Phys.* **60** 1129
Grüner G, Zawadowski A and Chaikin P M 1981 *Phys. Rev. Lett.* **46** 511
Grüner G and Zettl A 1985 *Phys. Rep.* **119** 117
Hansen L K and Carneiro K 1984 *Solid State Commun.* **49** 531
Horovitz B 1986 *Solitons* ed S E Trullinger, V E Zakharov and V L Pokrovsky (Amsterdam: North-Holland) p 691
Horovitz B and Trullinger S E 1984 *Solid State Commun.* **49** 195
Kaup D J and Newell A C 1978 *Proc. R. Soc.* A **361** 413
Kivshar Yu S, Konotop V V and Sinitsyn Yu A 1986 *Z. Phys.* B **65** 209
Krive I V, Rozhavsky A S and Kulik I O 1986 *Fiz. Nizk. Temp.* **12** 1123
Krive I V, Rozhavsky A S and Rubakov V A 1987 *Zh. Eksp. Teor. Fiz. Pis. Red.* **46** 99
Lee P A and Rice T M 1979 *Phys. Rev.* B **19** 3970
Lee P A, Rice T M and Anderson P W 1974 *Solid State Commun.* **14** 703
Maki K 1977 *Phys. Rev. Lett.* **39** 46

Maki K 1978 *Phys. Rev.* B **18** 1641
Malomed B A 1984 *Phys. Lett.* A **102** 83
—— 1985 *Physica* D **15** 385
—— 1987a *Phys. Lett.* **120A** 28
—— 1987b *Physica* D **27** 113
—— 1988 *J. Phys. C: Solid State Phys.* **21** 5163
—— 1989 *Phys. Rev.* B **39** 8018
Malomed B A and Ustinov A V 1990 *Phys. Rev.* B **41** 254
McLaughlin D W and Scott A C 1978 *Phys. Rev.* A **18** 1652
Mineev M B, Feigelman M V and Shmidt V V 1981 *Zh. Eksp. Teor. Fiz.* **81** 290
Olsen O H and Samuelsen M R 1984 *Phys. Rev.* B **29** 2803
Rice M J, Bishop A R, Krumhansl J A and Trullinger S E 1976 *Phys. Rev. Lett.* **36** 432
Sakai S, Samuelsen M R and Olsen O H 1987 *Phys. Rev.* B **36** 217
Weger M and Horovitz B 1982 *Solid State Commun.* **43** 583
Zakharov V E, Manakov S V, Novikov S P and Pitaevsky L P 1980 *Theory of Solitons* (Moscow: Nauka)
Ziman J M 1979 *Models of Disorder* (Cambridge: Cambridge University Press)